Journal of Zhejiang University-SCIENCE C (Computers & Electronics)
ISSN 1869-1951 (Print); ISSN 1869-196X (Online)
www.zju.edu.cn/jzus; www.springerlink.com
E-mail: jzus@zju.edu.cn

Time-dependent changes in eye-specific segregation in the dorsal lateral geniculate nucleus and superior colliculus of postnatal mice*

Yu-qing CHEN#, Yu-pu DIAO#, Jing-gang DUAN, Li-yuan CUI, Jia-yi ZHANG†‡

(*Institutes of Brain Science and State Key Laboratory of Medical Neurobiology, Fudan University, Shanghai 200032, China*)

†E-mail: jiayizhang@fudan.edu.cn

Received Apr. 26, 2014; Revision accepted July 24, 2014; Crosschecked Sept. 17, 2014

Abstract: Eye-specific segregation in the dorsal lateral geniculate nucleus (dLGN) and superior colliculus (SC) starts from the embryonic stage and continues to develop postnatally until eye-opening in mice. However, there have been few systematic studies on the details of this developmental process. Here, we carried out time-dependent studies of eye-specific segregation in the dLGN and SC. Our results demonstrated that the development of eye-specific segregation in the SC is completed before postnatal day 12 (P12), which is earlier than in the dLGN (P20). During the whole period, ipsilateral and overlapping axonal projections decreased continuously in both the dLGN and SC. On the other hand, contralateral axonal projections showed little change, except for a slight decrease between P8 and P20 in the dLGN.

Key words: Eye segregation, Dorsal lateral geniculate nucleus (dLGN), Superior colliculus, Mouse visual system
doi:10.1631/jzus.C1400153 **Document code:** A **CLC number:** TP183; Q42

1 Introduction

The visual pathway is a popular model for studying the wiring mechanism of neural circuits (Blankenship and Feller, 2010). Recently, the mouse visual system has been intensively studied to explore the principles of neural circuit formation (Huberman and Niell, 2011; Wei *et al.*, 2011; Brooks *et al.*, 2013). Several pathways from retinal ganglion cells (RGCs) have been found in the mouse visual system but there are two major pathways. One pathway goes to the dorsal lateral geniculate nucleus (dLGN), namely the retinogeniculate pathway. The other goes to the superior colliculus (SC), namely the retinocolliculus pathway.

Despite being intensively studied, many features of these two pathways are not well documented, including the development of eye-specific segregation. Previous studies showed that RGC axons from the two eyes are intermingled in the dLGN shortly after birth and become segregated into distinct areas by P12–P14, just at the onset of vision in mice (Jaubert-Miazza *et al.*, 2005). However, there are few reports on the detailed development of eye-specific segregation in both the dLGN and SC. In this study, we explored precise eye-specific projection patterns at different ages within the first three postnatal weeks using the same tracers and quantification methods. Our results provide a basic reference for further research on eye-specific segregation in mice.

‡ Corresponding author
# These two authors contributed equally to this work

* Project supported by the Shanghai Postdoctoral Scientific Program, the National Natural Science Foundation of China (No. 31271158), the Doctoral Program of Higher Education from Ministry of Education of China, the Innovation Program of Shanghai Municipal Education Commission (No. 13ZZ002), the Shanghai Municipal Commission of Health and Family Planning, Science and Technology Commission of Shanghai Municipality (Nos. 12ZR1441000 and 13PJ1401000), and the Young 1000 Plan

2 Materials and methods

2.1 Animals

All animal care and experiments were performed in accordance with the Fudan University Shanghai Medical College guidelines. C57BL/6 mice were obtained from the Slac Laboratory Animal Co. and kept in a mouse facility at 22 °C and relative humidity 50%, with 12 h light and 12 h dark cycles.

2.2 Intravitreous injection

Mice at different ages were deeply anesthetized using ice or isoflurane (3%) in oxygen. 1.2 μl of 2 μg/μl Alexa fluor488-conjugated cholera toxin, short for CTB-488 (green) (Molecular Probes, Invitrogen, C22841) and CTB-555 (red) (Molecular Probes, Invitrogen, C22843) were injected into the left and right eyes using the Nanoject II system (Drummond Scientific Company). Injected mice were perfused 48 h later.

For dye-testing experiments, the injection procedure was the same as above and the perfusion times were 48 h, 96 h, or 144 h post injection.

2.3 Image acquisition

After intravitreous injection, mice were perfused and their brains fixed in 4% paraformaldehyde (PFA) overnight. The brains were sectioned into 100 μm slices for dLGN examination in the coronal direction and 120 μm slices for SC examination in the sagittal direction using a vibratome (1000VT, Leica) machine. For the dLGN, four slices containing the largest dLGNs were collected. For the SC, four consecutive slices starting from 120 μm lateral to the midline were collected. Images were taken using a BX51 (Olympus) microscope.

2.4 Image analysis

Eye-specific segregation (contralateral and ipsilateral projections) was quantified according to the protocols of Xu *et al.* (2011). All images were background subtracted using ImageJ analysis. Contralateral and ipsilateral fractions were calculated using a custom Matlab program. The areas of the dLGN and SC were outlined manually according to green contralateral fluorescent signals. For consistency, the same person performed the outlining of the territories. The ratio of contralateral and ipsilateral projections was then calculated as the fraction of green and red pixels in the defined territory. The overlapping fraction refers to the fraction of pixels that were both red and green. The fractions of contralateral and ipsilateral projections were calculated based on a series of thresholds. We chose pixels with intensities larger than 10% of the maximum intensity for further analysis, because this condition best described the segregation phenomenon. For the SC, there were several steps before background subtraction: two images of the SC were merged to obtain a complete SC, and then the SC images acquired from red and green channels were stacked and cropped into images of the same size. These images were then used for the background subtraction and pixel threshold calculations.

The quantified dLGN or SC slices were averaged for each mouse. For each time point, we collected three mice from different mothers in parallel experiments for SC and at least five mice for dLGN analysis.

3 Results

3.1 Visualization of axon pruning with CTB-Alexa dyes

To test whether the two fluorescent dyes could detect dynamic developmental changes over time, we conducted intraocular injection experiments at P2, P4, and P6. These mice were perfused at P8 (Fig. 1a). The analyzed fractions in the dLGN at P2, P4, and P6 were 0.925, 0.917, and 0.933, respectively (n=1, Fig. 1b) for contralateral axons, 0.255, 0.219, and 0.216, respectively (n=1, Fig. 1c) for ipsilateral fractions, and 0.218, 0.17, and 0.18, respectively (n=1, Fig. 1d) for overlapping fractions. Among the three mice injected at different ages, the morphology and size of contralateral, ipsilateral, and overlapping projections in the dLGN were similar. The result demonstrated that CTB-488 and CTB-555 could anterogradely label RGC terminals in the dLGN and SC for detecting eye-specific segregation. These results further demonstrated that these dyes could retract with the axon terminals. Therefore, the CTB-Alexa dye-labeling method is useful for exploring the detailed developmental changes in retinogeniculate axons.

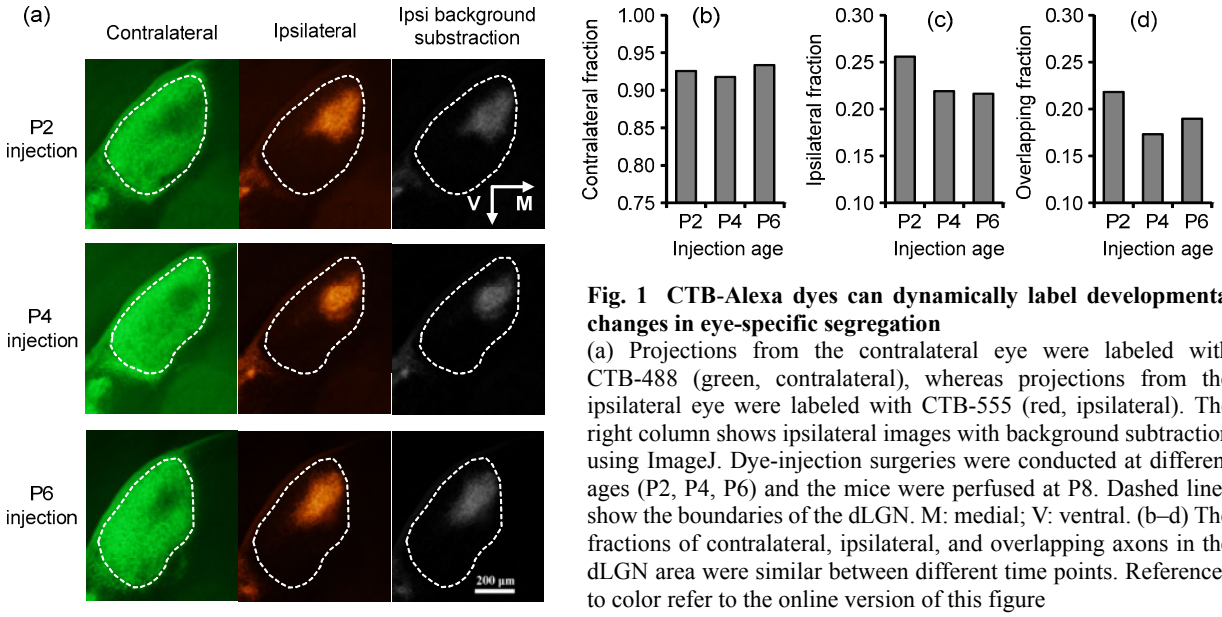

Fig. 1 CTB-Alexa dyes can dynamically label developmental changes in eye-specific segregation

(a) Projections from the contralateral eye were labeled with CTB-488 (green, contralateral), whereas projections from the ipsilateral eye were labeled with CTB-555 (red, ipsilateral). The right column shows ipsilateral images with background subtraction using ImageJ. Dye-injection surgeries were conducted at different ages (P2, P4, P6) and the mice were perfused at P8. Dashed lines show the boundaries of the dLGN. M: medial; V: ventral. (b–d) The fractions of contralateral, ipsilateral, and overlapping axons in the dLGN area were similar between different time points. References to color refer to the online version of this figure

3.2 Retinogeniculate axons from the two eyes segregate over time

We next examined eye-specific segregation in the dLGN at different ages (P3–4, P5–6, P8–9, P20–21, Fig. 2, Table 1). The contralateral fractions went from 0.910±0.024 at P3–4 to 0.940±0.012 at P8–9, but decreased to 0.851±0.016 at P20–21 (Figs. 2a and 2b). The fractions at P20–21 were significantly different from those of the other two ages (P=0.007 between P8–9 and P20–21, and P=0.021 between P5–6 and P20–21, Student's t-test). The development pattern of the ipsilateral and overlapping fractions was quite different from that of the contralateral fractions (Figs. 2a, 2c, and 2d). At P3–4, the RGC axons from the two eyes were not well separated and eye-specific projection patterns were still immature. The ipsilateral fraction was 0.747±0.026 (n=5, Figs. 2a and 2c). Compared to P3–4, ipsilateral fractions at P8-9 were reduced 2.7 fold to 0.273±0.028 (n=7, Fig. 2c). After eye opening at P20-21, the ipsilateral fractions further decreased to 0.179±0.009 (n=6, Fig. 2c). There were significant differences between P3–4 and P5–6, P5–6 and P8–9, P8–9 and P20–21 (P=0.007, 0.003, 0.010, respectively, Student's t-test). The way that the overlapping fractions changed over time followed a similar trend to that of the ipsilateral fractions (Fig. 2d). The differences for overlapping fractions also varied between P3–4 and P5–6, P5–6 and P8–9, P8–9 and P20–21 (P=0.042, 0.003, 0.003, respectively, Student's t-test).

Table 1 Summary of quantified eye-specific segregation in the dLGN

Age	Contralateral fraction	Ipsilateral fraction	Overlapping fraction
P3–4 (n=5)	0.910±0.024	0.747±0.026	0.699±0.039
P5–6 (n=7)	0.928±0.016	0.581±0.043	0.554±0.041
P8–9 (n=7)	0.940±0.012	0.273±0.028	0.245±0.026
P20–21 (n=6)	0.851±0.016	0.179±0.009	0.118±0.004

3.3 Development of eye-specific segregation in the SC

We then examined eye-specific segregation in the SC (Fig. 3a). The ipsilateral fractions decreased during the whole period from 0.165±0.018 (P3–4, n=3) to 0.022±0.008 (P7–8, n=3) and to 0.00037±0.0002 (P11–12, n=3) (Table 2, Fig. 3c). There were significant differences in ipsilateral fractions between P3–4 and P7–8, P=0.0078 and between P7–8 and P11–12, P=0.039 (Fig. 3c). The trend for the change in overlapping fractions was similar to that of the ipsilateral fractions, but with a slightly smaller ratio (Table 2, Fig. 3d). Unlike the ipsilateral and overlapping fractions, no obvious change was observed in the contralateral fraction (Table 2, Fig. 3b). Analysis of the data using Student's t-test showed that there was no significant difference in the overlapping and contralateral fractions between P7–8 and P11–12, which further demonstrated that the development of

contralateral projections is almost complete by P7–8. The data described here indicate that, during the whole course of development, contralateral projections occupied the dominant portion of the SC, and the change in the contralateral portion was less than 10%. In contrast, the ipsilateral and overlapping fractions decreased rapidly.

Table 2 Summary of quantified eye-specific segregation in the SC

Age	Contralateral fraction	Ipsilateral fraction	Overlapping fraction
P3–4 (n=3)	0.798±0.023	0.165±0.018	0.139±0.016
P7–8 (n=3)	0.885±0.018	0.022±0.008	0.018±0.010
P11–12 (n=3)	0.807±0.161	0.00037±0.0002	0.00028±0.00016

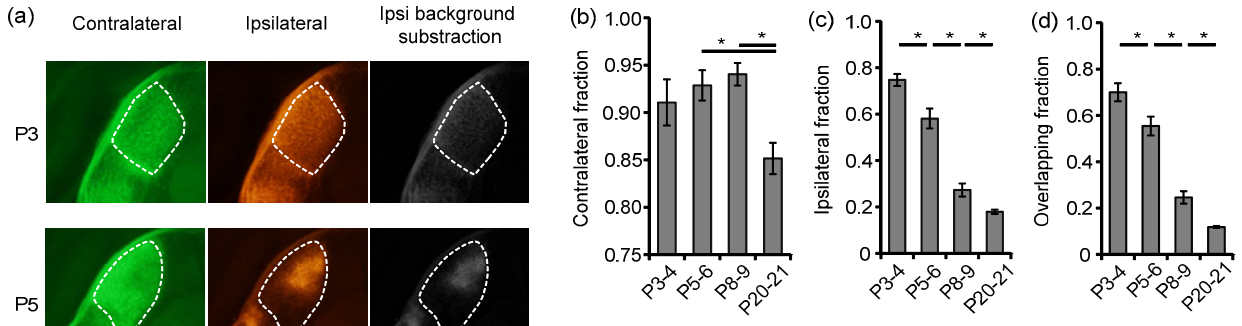

Fig. 2 Age-dependent eye-specific segregation of retinogeniculate projections in the mouse dLGN

(a) CTB-488 and CTB-555 were injected into left and right eyes respectively to visualize the RGC projecting axons at 1–2, 3–4, 7–8, and 19–20 days postnatal. Mice were perfused 48 h later. The coronal images show contralateral, ipsilateral, and background-subtracted ipsilateral projections at P3, P5, P8, and P20, respectively. Dashed lines show the boundaries of the dLGNs. (b–d) The histogram represents quantified contralateral, ipsilateral, and overlapping fractions of the dLGN area using the Matlab program. The retinogeniculate projections from the ipsilateral eye decreased continuously and significantly until P20, while fractions of contralateral axons remained relatively stable. $^{*}P$<0.05 (Student's t-test). Error bars represent the S.E.M.

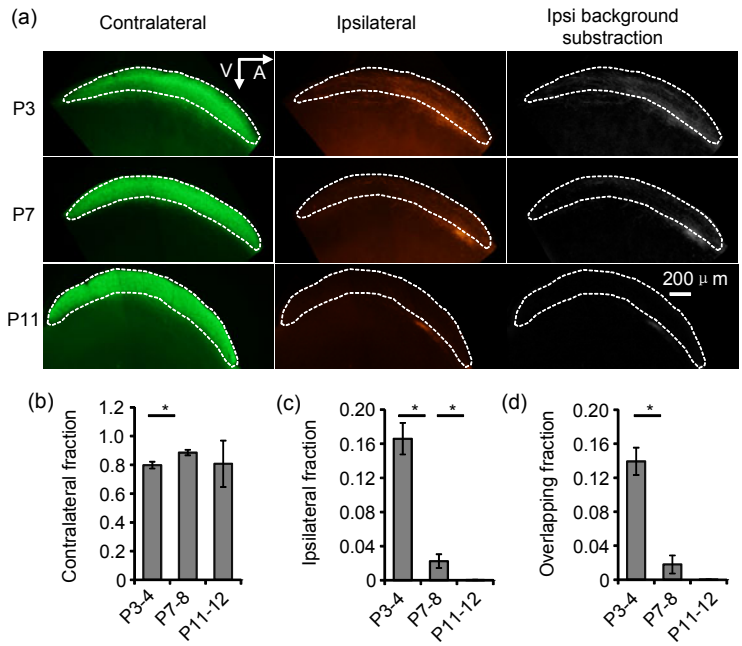

Fig. 3 Age-dependent eye-specific segregation of retinocolliculus projections in the mouse superior colliculus

(a) 48 h after intraocular injection, the mice were perfused and their brains fixed overnight and sectioned sagittally. At P3, RGC axons from the ipsilateral eye to the SC were widely distributed. (b–d) The histograms show contralateral, ipsilateral, and overlapping fractions of the SC area. The fraction of ipsilateral axons continued to decrease markedly on subsequent days, and then tended to stabilize. Dashed lines show the boundaries of the contralateral superior colliculus. * P<0.05 (Student's t test). Error bars represent the S.E.M. A: anterior; V: ventral

4 Discussion

Here, we studied the development of eye-specific segregation of the dLGN and SC using the same tracer and quantification methods. Our experiments demonstrated that during the first postnatal week, ipsilateral fractions decreased dramatically in the dLGN, while contralateral fractions changed only slightly. As a result, the overlapping fractions also decreased a lot. By around P9, the pattern of eye-segregation had already formed. From P9 to P21, we observed a sudden decrease in contralateral fractions. At the same time, ipsilateral fractions decreased. The contralateral and ipsilateral fractions are 'retracted' from their previous areas, so the overlapping fractions also decreased. Therefore, there are two stages during the course of development of eye-specific segregation in the dLGN: a rapid stage of pattern formation (P3–P9), followed by a slow stage of further segregation (P9–P21). The development of eye-specific segregation in the mouse visual system is determined by both neuronal activity and axon-guidance molecules (Hanson and Landmesser, 2004; Bouzioukh *et al.*, 2006; Huberman *et al.*, 2008). The molecules guide the positioning of the axon terminals, while the neuronal activity, especially the retinal wave, is one of the most important driving forces for the refinement of eye-specific segregation (Butts *et al.*, 2007). Disrupting RGC activities before eye-opening lead to defects in eye-specific segregation development in the dLGN (Rossi *et al.*, 2001) and SC (Zhang *et al.*, 2012). The timing of the rapid and slow developmental stages is coincident with those of stage II and stage III retinal waves (P20 is at the end of the stage III retinal wave, Bansal *et al.*, 2000; Demas *et al.*, 2003). Therefore, the stage II retinal wave may be responsible for pruning of the neuron terminals in the dLGN. Visual input starts during the slow developmental stage. It is likely that stage III retinal waves and visual experience both guide further eye-specific segregation.

In the SC, the ipsilateral fractions decreased and the contralateral fractions changed only slightly between P3 and P12. As a result, the overlapping fractions also decreased during the whole period. Similar to the dLGN, there are two stages during eye-specific segregation in the SC. The pattern formation stage is in the first postnatal week. By P8, the axons from the ipsilateral eye had already formed target zones. This is consistent with previous studies (Furman *et al.*, 2013). From P8 to P12, the ipsilateral axons went through further eye-specific segregation. The development of eye-specific segregation in the SC was faster than in the dLGN. Moreover, the ipsilateral fractions in the SC were much smaller than those in the dLGN, but the reasons for this are still unclear. Application of new approaches, such as optogenetics, in neuroscience may lead to novel results (Deisseroth, 2011).

Acknowledgements

Yu-pu DIAO, Yu-qing CHEN, and Jia-yi ZHANG designed the experiment. Yu-pu DIAO, Yu-qing CHEN, and Li-yuan CUI conducted surgery experiments and data analysis. Jing-gang DUAN was responsible for image acquisition. We thank all members of the laboratory for discussion.

References

Bansal, A., Singer, J.H., Hwang, B.J., *et al*., 2000. Mice lacking specific nicotinic acetylcholine receptor subunits exhibit dramatically altered spontaneous activity patterns and reveal a limited role for retinal waves in forming ON and OFF circuits in the inner retina. *J. Neurosci.*, **20**(20): 7672-7681.

Blankenship, A.G., Feller, M.B., 2010. Mechanisms underlying spontaneous patterned activity in developing neural circuits. *Nat. Rev. Neurosci.*, **11**(1):18-29. [doi:10.1038/nrn2759]

Bouzioukh, F., Daoudal, G., Falk, J., *et al*., 2006. Semaphorin3A regulates synaptic function of differentiated hippocampal neurons. *Eur. J. Neurosci.*, **23**(9):2247-2254. [doi:10.1111/j.1460-9568.2006.04783.x]

Brooks, J.M., Su, J., Levy, C., *et al*., 2013. A molecular mechanism regulating the timing of corticogeniculate innervation. *Cell Reports*, **5**(3):573-581. [doi:10.1016/j.celrep.2013.09.041]

Butts, D.A., Kanold, P.O., Shatz, C.J., 2007. A burst-based "Hebbian" learning rule at retinogeniculate synapses links retinal waves to activity-dependent refinement. *PLoS Biol.*, **5**(3):e61. [doi:10.1371/journal.pbio.0050061]

Deisseroth, K., 2011. Optogenetics. *Nat. Methods*, **8**(1):26-29. [doi:10.1038/nmeth.f.324]

Demas, J., Eglen, S.J., Wong, R.O., 2003. Developmental loss of synchronous spontaneous activity in the mouse retina is independent of visual experience. *J. Neurosci.*, **23**(7): 2851-2860.

Furman, M., Xu, H.P., Crair, M.C., 2013. Competition driven by retinal waves promotes morphological and functional synaptic development of neurons in the superior colliculus. *J. Neurophysiol.*, **110**(6):1441-1454. [doi:10.1152/jn.01066.2012]

Hanson, M.G., Landmesser, L.T., 2004. Normal patterns of spontaneous activity are required for correct motor axon guidance and the expression of specific guidance molecules. *Neuron*, **43**(5):687-701. [doi:10.1016/j.neuron.2004.08.018]

Huberman, A.D., Niell, C.M., 2011. What can mice tell us about how vision works? *Trends Neurosci.*, **34**(9):464-473. [doi:10.1016/j.tins.2011.07.002]

Huberman, A.D., Feller, M.B., Chapman, B., 2008. Mechanisms underlying development of visual maps and receptive fields. *Ann. Rev. Neurosci.*, **31**(1):479-509. [doi:10.1146/annurev.neuro.31.060407.125533]

Jaubert-Miazza, L., Green, E., Lo, F.S., *et al*., 2005. Structural and functional composition of the developing retinogeniculate pathway in the mouse. *Vis. Neurosci.*, **22**(5):661-676. [doi:10.1017/S0952523805225154]

Rossi, F.M., Pizzorusso, T., Porciatti, V., *et al*., 2001. Requirement of the nicotinic acetylcholine receptor beta 2 subunit for the anatomical and functional development of the visual system. *PNAS*, **98**(11):6453-6458. [doi:10.1073/pnas.101120998]

Wei, W., Hamby, A.M., Zhou, K., *et al*., 2011. Development of asymmetric inhibition underlying direction selectivity in the retina. *Nature*, **469**(7330):402-406. [doi:10.1038/nature09600]

Xu, H.P., Furman, M., Mineur, Y.S., *et al*., 2011. An instructive role for patterned spontaneous retinal activity in mouse visual map development. *Neuron*, **70**(6):1115-1127. [doi:10.1016/j.neuron.2011.04.028]

Zhang, J., Ackman, J.B., Xu, H.P., *et al*., 2012. Visual map development depends on the temporal pattern of binocular activity in mice. *Nat. Neurosci.*, **15**(2):298-307. [doi:10.1038/nn.3007]